

Light hadron spectroscopy with two flavors of $O(a)$ improved dynamical quarks *

JLQCD Collaboration: S. Aoki^a, R. Burkhalter^{a,b}, M. Fukugita^c, S. Hashimoto^d, K-I. Ishikawa^d, N. Ishizuka^{a,b}, Y. Iwasaki^{a,b}, K. Kanaya^{a,b}, T. Kaneko^d, Y. Kuramashi^d, M. Okawa^d, T. Onogi^e, S. Tominaga^b, N. Tsutsui^d, A. Ukawa^{a,b}, N. Yamada^d, and T. Yoshié^{a,b}.

^aInstitute of Physics, University of Tsukuba, Tsukuba, Ibaraki 305-8571, Japan

^bCenter for Computational Physics, University of Tsukuba, Tsukuba, Ibaraki 305-8577, Japan

^cInstitute for Cosmic Ray Research, University of Tokyo, Kashiwa 277-8582, Japan

^dHigh Energy Accelerator Research Organization (KEK), Tsukuba, Ibaraki 305-0801, Japan

^eDepartment of Physics, Hiroshima University Higashi-Hiroshima, Hiroshima 739-8526, Japan

We report on our study of light hadron spectrum and quark masses in QCD with two flavors of dynamical quarks. Simulations are made with the plaquette gauge action and the non-perturbatively $O(a)$ improved Wilson quark action. We simulate 5 sea quark masses corresponding to $m_{PS}/m_V \simeq 0.8-0.6$ at $\beta = 5.2$ on $12^3 \times 48$, $16^3 \times 48$ and $20^3 \times 48$ lattices. A comparison with previous calculations in quenched QCD indicates sea quark effects in meson and quark masses.

1. Introduction

One of the major goals of lattice QCD simulation is to confirm the validity of QCD as the theory of strong interaction in the low energy region by comparing its prediction for the hadron spectrum to experiment. Because of huge computational demand to perform simulations with dynamical quarks, however, many works have been forced to neglect effects of dynamical sea quarks. In this quenched approximation, the CP-PACS collaboration found some deviation in the light hadron spectrum from experiment[1], which motivates us to investigate sea quark effects by performing simulations of QCD with the realistic number of dynamical quark flavors.

The JLQCD collaboration started numerical simulations of dynamical QCD on a supercomputer Hitachi SR8000 model F1, which is newly installed at KEK on March 2000. It has a 1.2 TFlops of peak performance and provides about 400 sustained GFlops for our simulation code. We carry out simulations of QCD with two flavors

of dynamical quarks and investigate the chiral extrapolation and finite size effects in the light hadron spectrum, as a step toward studies of QCD with 2+1 flavors (i.e. u, d plus s quarks).

2. Simulations

We study QCD with two degenerate flavors of dynamical quarks, which are identified with u and d quarks; the strange quark is treated in the quenched approximation. We employ the $O(a)$ improved quark action[3] with the clover coefficient c_{SW} determined non-perturbatively by the ALPHA collaboration[4]. Simulations are performed at $\beta = 5.2$ and $c_{SW} = 2.02$, for which a^{-1} evaluated at the physical mass of dynamical ud quarks is approximately 2 GeV and hence scaling violation is not expected to be too large. We simulate 5 sea quark masses in the range $m_{PS}/m_V \simeq 0.8-0.6$. Since finite size effects could be more important with dynamical quarks, we perform simulations on three lattices with different spatial sizes, $12^3 \times 48$, $16^3 \times 48$ and $20^3 \times 48$. We have accumulated 3000 thermalized HMC tra-

*Talk presented by T. Kaneko

Table 1

Simulation parameters. We also list the lattice spacing a_{r_0} fixed by $r_0 = 0.49$ fm for $16^3 \times 48$ lattices.

lattice	K_{sea}	#traj.	m_{PS}/m_V	a_{r_0} [fm]
$16^3 \times 48$	0.1340	3000	0.802(4)	0.1288(10)
	0.1343	3000	0.781(6)	0.1201(10)
	0.1346	3000	0.743(6)	0.1127(7)
	0.1350	3000	0.714(9)	0.1084(7)
	0.1355	3000	0.596(18)	0.1006(5)
$12^3 \times 48$	0.1346	3000	0.735(9)	–
	0.1350	3000	0.695(15)	–
$20^3 \times 48$	0.1346	2000	0.756(8)	–
	0.1350	2800	0.706(9)	–

jectories on the $16^3 \times 48$ lattice, while simulations on other lattices are in progress. Other details of simulation parameters are summarized in Table 1.

3. Static quark potential

We calculate the static quark potential on the $16^3 \times 48$ lattice using the smeared Wilson loops. Since we do not observe any signal of flattening of the potential due to string breaking, potential data are parameterized with the form

$$V(\mathbf{r}) = V_0 - \alpha/|\mathbf{r}| - g \cdot \delta V(\mathbf{r}) + \sigma \cdot |\mathbf{r}|, \quad (1)$$

where $\delta V(\mathbf{r}) = (G(\mathbf{r}) - 1/|\mathbf{r}|)$ represents a correction to the short-distance Coulomb term calculated with the lattice gluon propagator[5]. Figure 1 shows a plot obtained for the heaviest sea quark mass, where we find that deviation of the potential data from the fit curve is at most 1% in the fitting range of \mathbf{r} . We determine the Sommer scale r_0 [6] from the parameterization (1). The lattice spacing determined with the condition $r_0 = 0.49$ fm is listed in Table 1.

4. Light meson mass measurement

We calculate light hadron correlators for 6 values of the valence quark masses in the range $m_{\text{PS}}/m_V \simeq 0.80-0.50$ for each sea quark mass. Measurements have been completed for the $16^3 \times 48$ lattice, while only the degenerate case ($K_{\text{val}} = K_{\text{sea}}$) is measured on $12^3 \times 48$ and $20^3 \times 48$. Most of the analysis results discussed in this talk are based on the $16^3 \times 48$ lattice data except for the finite size effect in the following.

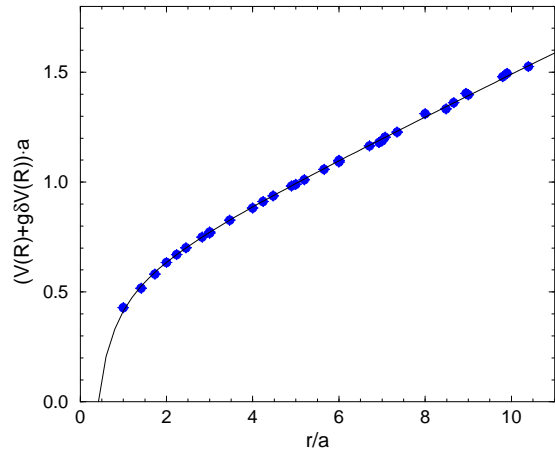


Figure 1. Corrected static quark potential $V(r) + g \cdot \delta V(r)$ at $K_{\text{sea}} = 0.1340$ on $16^3 \times 48$ lattice. The solid line represents the fitting curve (1).

Figure 2 shows the effective mass of degenerate ($K_{\text{val}} = K_{\text{sea}}$) pseudo-scalar meson at the second lightest sea quark mass. Data are shown for three different spatial volumes 12^3 , 16^3 and 20^3 . We find that the fitted masses on the two larger lattices are in good agreement with each other both for the pseudo-scalar and vector mesons, as shown in Figure 3. This is also observed for other lattices with heavier sea quarks. This suggests that finite size effects are already small for the 16^3 lattice. We are currently extending similar measurements to the lightest sea quark $K_{\text{sea}} = 0.1355$, for which finite size effects are expected to be more important.

5. Sea quark effect in meson masses

Figure 4 shows the vector meson mass as a function of the pseudo-scalar meson mass squared. Since the effective lattice spacing decreases as the sea quark mass becomes smaller, which complicates the chiral extrapolation if made using the lattice unit, we plot the meson masses normalized by a physical quantity r_0 measured for each sea quark mass. We also plot the quenched data [7] in Figure 4, where we clearly see an indication of sea quark effect, i.e. slope in two-flavor QCD is significantly larger than that in quenched QCD. This leads to a larger hyperfine splitting of the strange meson as we shall see later. We also find that our results at different sea

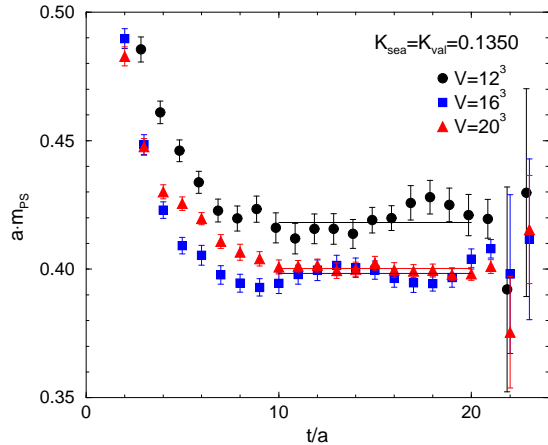


Figure 2. Effective masses for the pseudo-scalar meson at $K_{\text{sea}} = K_{\text{val}} = 0.1350$ on three different volumes. Solid lines represent the central value of the fit result.

quark masses lie almost on one curve. This indicates that the sea quark mass dependence of this quantity is not large in our simulated region of K_{sea} and more precise calculation is needed, particularly for the vector mesons, to see it clearly.

6. Chiral extrapolation

We employ two different strategies for the chiral extrapolation. In our main strategy, which we call method (A), we use meson and quark masses normalized by r_0 throughout the analysis. For instance, the pseudo-scalar meson mass squared is fit to the form

$$(m_{\text{PS}}r_0)^2 = A_s(m_{\text{sea}}r_0) + A_v(m_{\text{val}}r_0), \quad (2)$$

where m_{sea} and m_{val} are respectively sea and average valence quark masses defined through the vector Ward identity (VWI) relation $m_{q,\text{VWI}} = (1/K - 1/K_c)/2$. With this method, data is described very well by a simple linear fit. In the other strategy, method (B), we make the chiral extrapolation using meson and quark masses in the lattice unit. In this case, significant curvature is found in fits for both pseudo-scalar and vector meson masses, and therefore we have to introduce quadratic terms in the fitting function. We find that both fits give consistent results, although the fit error is generally larger for the method (B).

In each method, the physical quark masses m_{ud} and m_s are determined by tuning meson mass

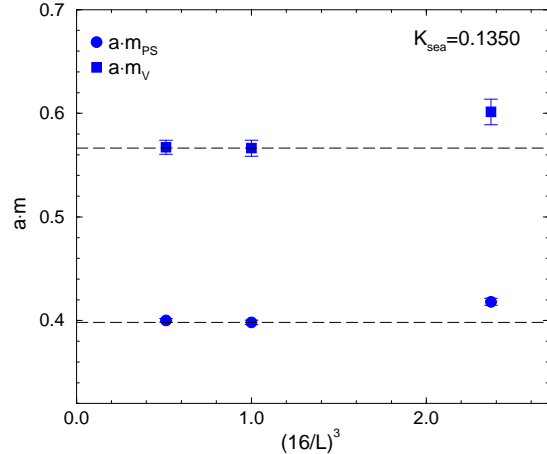


Figure 3. Fit results of pseudo-scalar (circles) and vector (squares) meson masses as a function of $(16/L)^3$. Results on $V = 16^3$ are shown also with dashed lines for a guide of eye.

ratios to their experimental values. We use m_π and m_ρ to fix m_{ud} and the lattice spacing. The strange quark mass m_s is determined from either m_K/m_ρ or m_ϕ/m_ρ .

Our results for the strange vector meson masses (K^* and ϕ), with pseudo-scalar (K) used to fix the strange quark mass, are shown in Figure 5 by filled circles (method (A)) or by filled squares (method (B)). For comparison, we also plot the CP-PACS data in the quenched approximation [1] and the recent two-flavor result [2]. A trend that the sea quark effect pushes up the vector meson masses toward the experimental values is seen in this plot.

7. Strange quark mass

The bare strange quark mass is calculated using either of two definitions, i.e. one from VWI and the other from the axial vector Ward identity (AWI), $2m_{q,\text{AWI}} = \langle \partial_4 A_4(t) P(0)^\dagger \rangle / \langle P(t) P(0)^\dagger \rangle$, where $A_\mu(t)$ and $P(t)$ are the axial vector current and pseudo-scalar density. We use the improved axial vector current $A_\mu^{(\text{imp})}(t) = A_\mu(t) + c_A \partial_\mu P(t)$, with c_A calculated at one-loop [8]. The continuum $\overline{\text{MS}}$ quark mass is obtained using one-loop matching [8,9] at scale $\mu = 1/a$ and evolved to $\mu = 2 \text{ GeV}$ with 3-loop β function [10].

Our results for the strange quark mass using

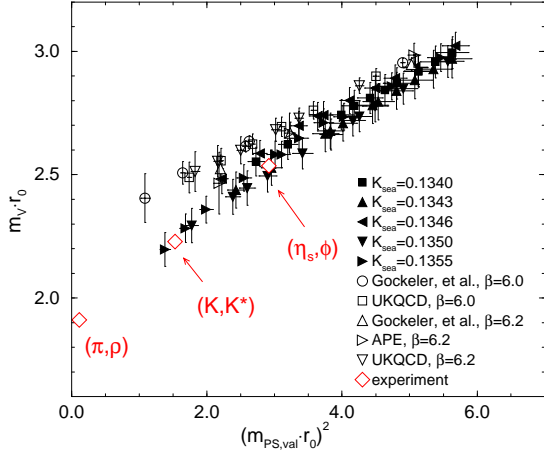


Figure 4. $(m_V r_0)$ vs $(m_{PS} r_0)^2$ in two flavor QCD (filled symbols). Open symbols represent results in quenched QCD in Refs. [7]. Experimental values are plotted with open diamonds using $r_0 = 0.49$ fm.

the method (A) are

$$m_s(2\text{GeV}) = \begin{cases} 94(2) \text{ MeV} & (\text{VWI}), \\ 88(3) \text{ MeV} & (\text{AWI}), \end{cases} \quad (3)$$

with K used as input, or

$$m_s(2\text{GeV}) = \begin{cases} 109(4) \text{ MeV} & (\text{VWI}), \\ 102(6) \text{ MeV} & (\text{AWI}), \end{cases} \quad (4)$$

with ϕ used as input. The method (B) gives consistent results.

Only the statistical errors are shown in (3) and (4). The systematic error is more significant, as indicated by the disagreement between VWI and AWI, and the difference between (3) and (4), although the latter is smaller than in the quenched results[1]. One of the most important sources of the systematic error is the use of the one-loop perturbative Z factor, for which a naive order counting gives $O(5\%)$. In addition, the discretization error of $O(a^2)$ or the quenching effect of the strange sea quark could also be important. A recent two-flavor simulation of CP-PACS predicted $m_s(2\text{GeV}) = 88_{-6}^{+4} \text{ MeV}$ or $90_{-11}^{+5} \text{ MeV}$ in the continuum limit with the K or ϕ used as input [2].

This work is supported by the Supercomputer project No.54 (FY2000) of High Energy Accelerator Research Organization (KEK), and also in part by the Grant-in-Aid of the Ministry of

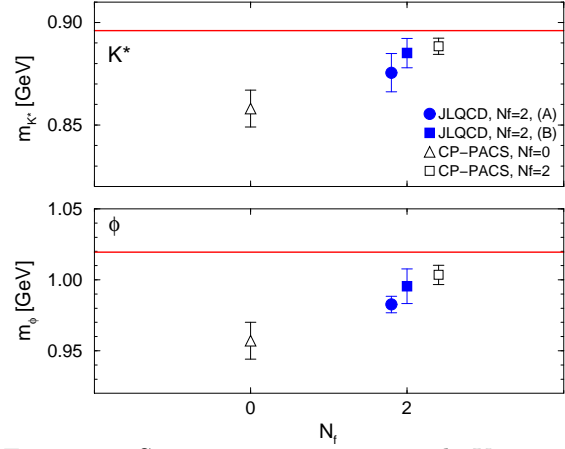


Figure 5. Strange meson masses with K -input. Filled circles and squares are our full QCD results using method (A) and (B), respectively. Open triangles and squares are CP-PACS's result in quenched[1] and full QCD[2]. Horizontal lines show experimental values.

Education (Nos. 10640246, 10640248, 11640250, 11640294, 11740162, 12014202, 12640253, 12640279 and 12740133). K-I.I, T.K and N.Y are supported by the JSPS Research Fellowship.

REFERENCES

1. S. Aoki *et al.* (CP-PACS Collaboration), Phys. Rev. Lett. 84 (2000) 238.
2. A. Ali Khan *et al.* (CP-PACS Collaboration), hep-lat/0004010; R. Burkhalter, in these proceedings.
3. B. Sheikholeslami and R. Wohlert, Nucl. Phys. B259 (1985) 572.
4. K. Jansen and R. Sommer, Nucl. Phys. B530 (1998) 185.
5. C. Michael, Phys. Lett. B283 (1992) 103.
6. R. Sommer, Nucl. Phys. B411 (1994) 839.
7. M. Gökeler *et al.*, Phys. Rev. D57 (1998) 5562; D. Becirevic *et al.*, hep-lat/9809129; UKQCD Collaboratin, Phys. Rev. D62 (2000) 054506.
8. M. Lüscher, P. Weisz, Nucl. Phys. B479 (1996) 429; S. Sint and P. Weisz, Nucl. Phys. B502 (1997) 251.
9. E. Gabrielli, *et al.*, Nucl. Phys. B362 (1991) 475.
10. O. V. Tarasov *et al.*, Phys. Lett. B 93 (1980) 429.